Supplementary Information

Effects of structural symmetry in cobalt porphyrin-electrocatalytic oxygen reduction reactions

*Yuqin Wei [a], Yongdi Liang [a], Qijie Wu [a], Zhaoli Xue [a], Lei Feng [b], Jianming Zhang [a], Long Zhao [a,] **

[a] School of Chemistry and Chemical Engineering, Jiangsu University, Zhenjiang, 212013, PR China.

[b] Monash Suzhou Research Institute, Monash University, Suzhou Industrial Park, Suzhou 215000, PR China

Corresponding author: longzhao@ujs.edu.cn

SI 1. Synthesis

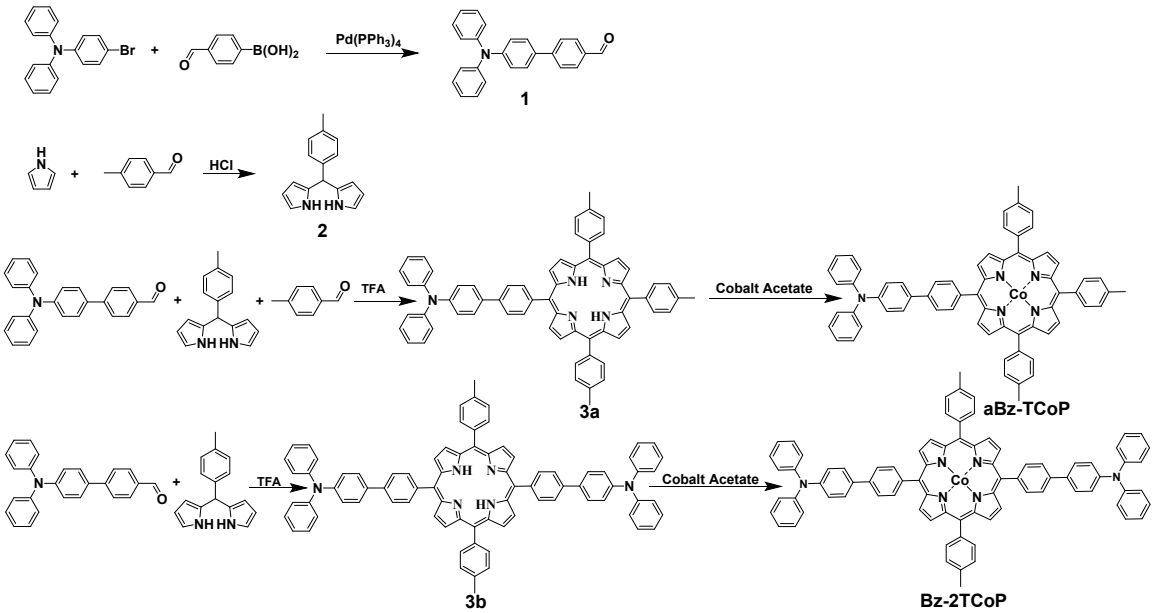

Figure S1. Synthetic routes for the investigated **aBz-TCoP** and **Bz-2TCoP**.

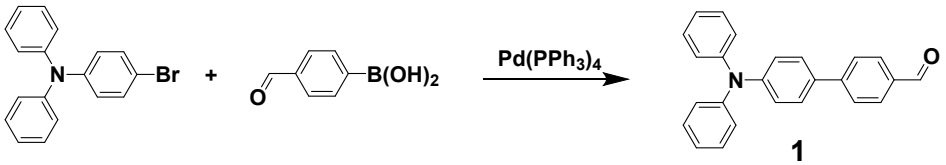

4'-(diphenylamino)-[1,1'-biphenyl]-4-carbaldehyde (Compound 1): 2 mmol 4-bromo-N, N-diphenylaniline, 2.2 mmol 4-formylphenylboronic acid, 0.1 mol tetrakis (triphenylphosphine) palladium, 10 mL THF, and 10 mL 0.4 M K_2CO_3 were mixed in a flask and the mixture was stirred for 12 h under dark and nitrogen atmosphere. A yellow solid was obtained by vacuum distillation and silica gel column chromatography (CH_2Cl_2: petroleum ether = 1:1). Yield: 91 %.

^{1}H NMR (400 MHz, Chloroform-*d*) δ 10.03 (s, 1H), 7.95 – 7.91 (m, 2H), 7.75 – 7.71 (m, 2H), 7.55 – 7.50 (m, 2H), 7.29 (dd, J = 8.5, 7.3 Hz, 4H), 7.17 – 7.13 (m, 6H), 7.08 (td, J = 7.3, 1.2 Hz, 2H).

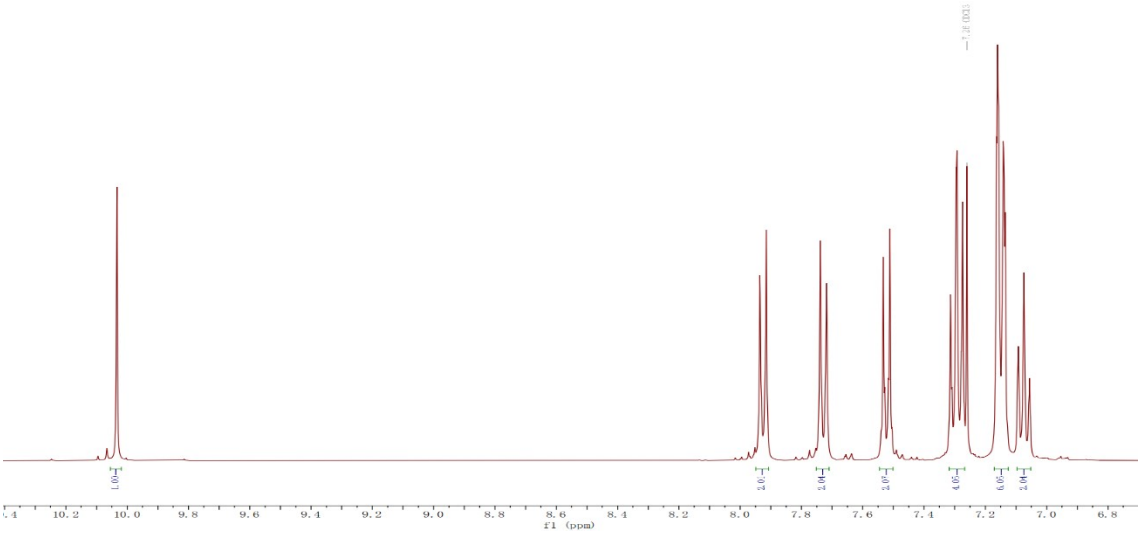

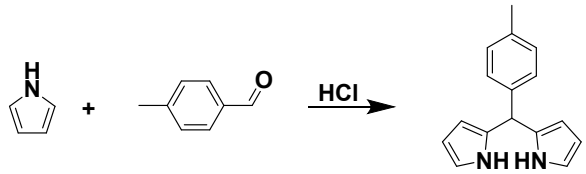

2

2,2'-(phenylmethylene)bis(1H-pyrrole) (Compound 2) was prepared following the method described in the literature [1].

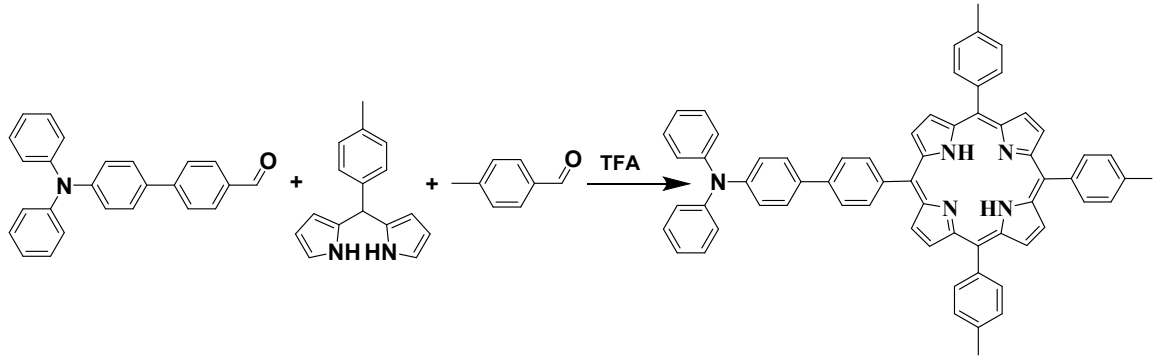

3a

N, N-diphenyl-4'-(5,15,20-tri-p-tolylporphyrin-10-yl)-[1,1'-biphenyl]-4-amine (Compound 3a): 1 mmol **Compound 1** (349.43 mg), 2 mmol **Compound 2** (472.26 mg) and 1 mmol *p*-methyl benzaldehyde (120.15 mg) were added to 100 mL anhydrous CH_2Cl_2. The mixture was stirred in a dark

and nitrogen atmosphere for 5 min, and then 2.42 mmol TFA (0.18 mL) was slowly added to initiate the reaction. After stirring at room temperature for 1 h, 1.5 mmol tetra-chloro-benzoquinone (393.3 mg) was added and stirred under the same condition. The reaction was monitored by thin-layer chromatography. Then 2.42 mmol TEA (0.337 mL) was added to neutralize the reaction. The crude product was purified by silica gel column chromatography (CH_2Cl_2: petroleum ether = 1:2) to obtain a purple solid. Yield: 8.6%.

^{1}H NMR (400 MHz, Chloroform-*d*) δ 8.92 (d, *J* = 4.8 Hz, 2H), 8.88 (d, *J* = 8.2 Hz, 6H), 8.28 – 8.24 (m, 2H), 8.11 (dd, *J* = 7.7, 1.3 Hz, 6H), 7.97 – 7.93 (m, 2H), 7.82 – 7.79 (m, 2H), 7.56 (d, *J* = 7.8 Hz, 6H), 7.35 (d, *J* = 7.2 Hz, 2H), 7.32 (d, *J* = 2.0 Hz, 2H), 7.31 – 7.28 (m, 2H), 7.25 – 7.21 (m, 4H), 7.12 – 7.06 (m, 2H), 2.71 (s, 9H), -2.73 (s, 2H).

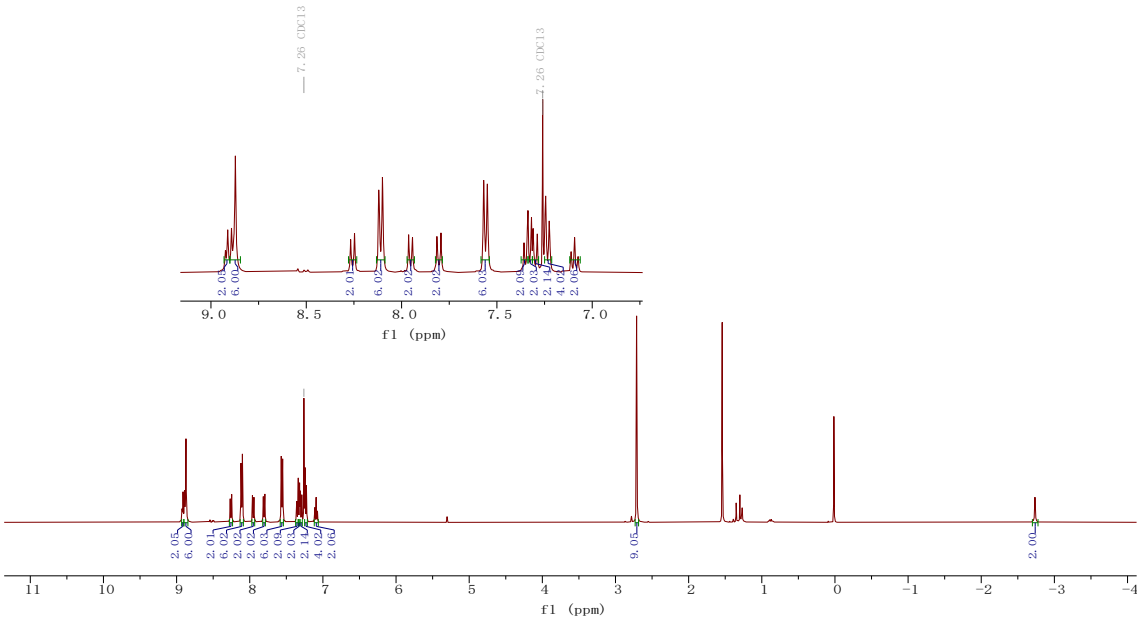

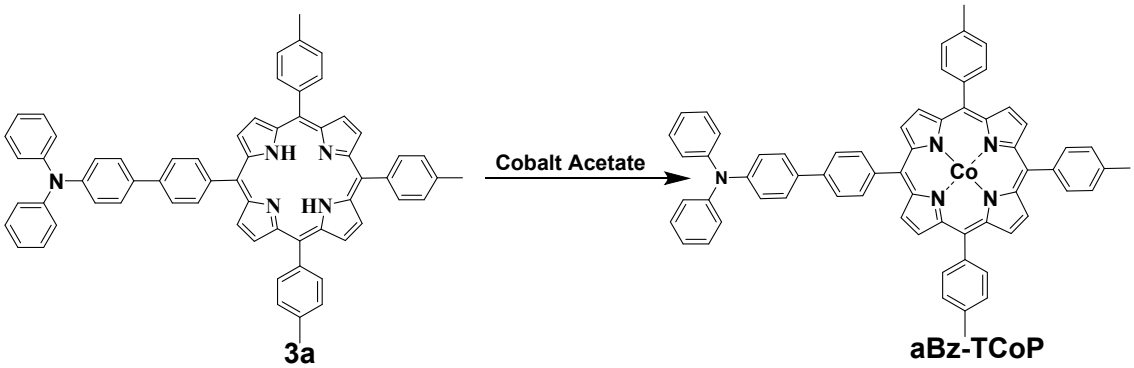

N, N-diphenyl-4'-(5,15,20-tri-p-tolylporphyrin-10-yl)-[1,1'-biphenyl]-4-amine cobalt (II)（aBz-TCoP）: 0.05 mmol **Compound 3a** (45.01 mg) was added to a double-necked bottle, and dissolved in the minimum volume of $CHCl_3$. The solution was refluxed at 68 °C for 15 min in a dark nitrogen atmosphere. Then 0.25 mmol cobalt acetate tetrahydrate (62 mg) in methanol was added to the bottle with a syringe. The mixture was continued to reflux, and the reaction was monitored by TLC. The organic phase was collected by extraction with CH_2Cl_2 and water, and was dried with anhydrous sodium sulfate and purified by silica gel column chromatography (CH_2Cl_2: petroleum ether = 1: 2) to obtain a dark red solid. Yield: 91%.

HR-MS (m/z): requires for: $C_{56}H_{47}CoN_5$ 956.3163, found $[M]^+$ = 956.3130

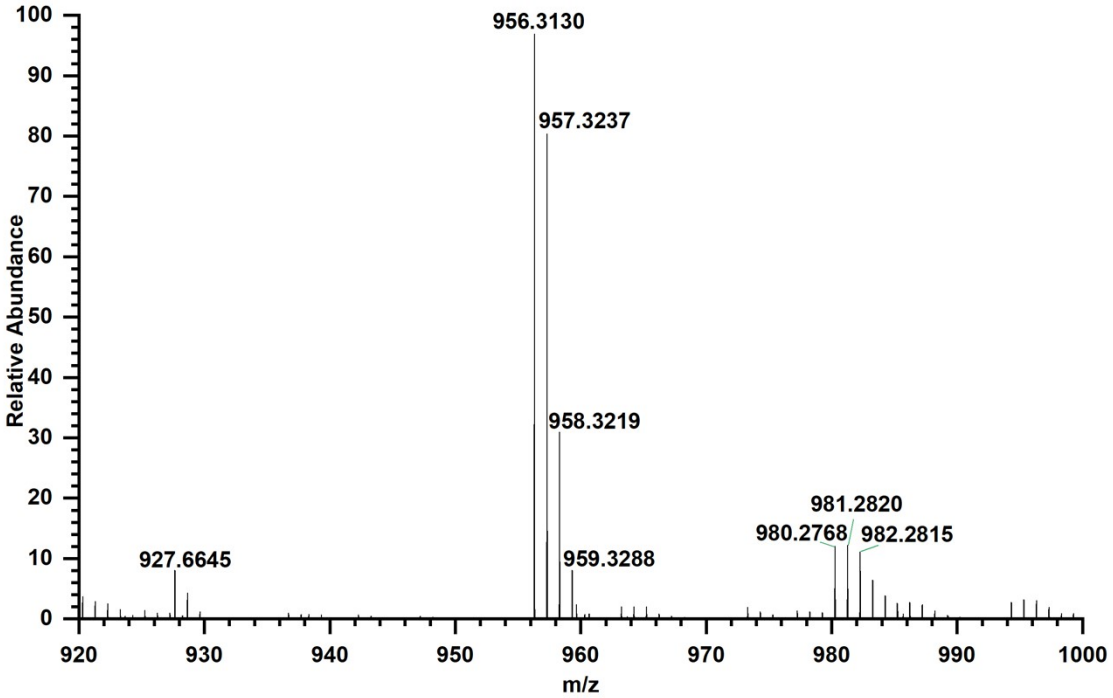

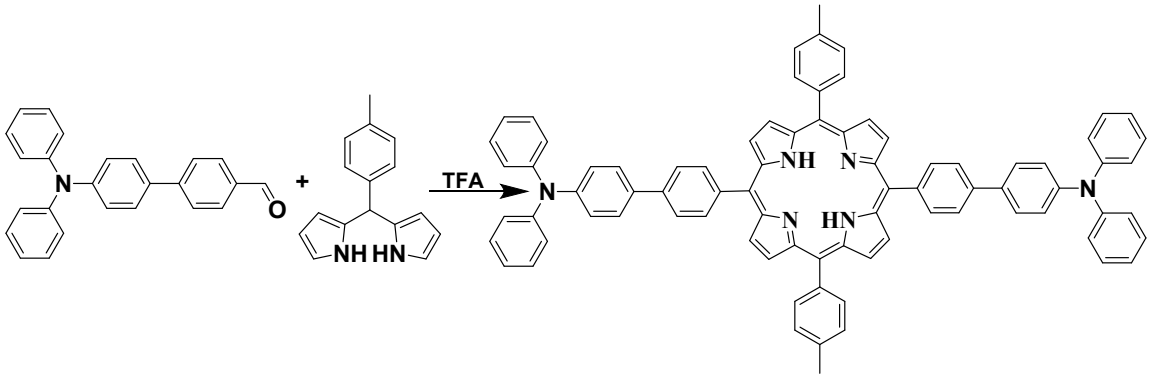

3b

4',4'''-(5,15-di-p-tolylporphyrin-10,20-diyl) bis (N, N-diphenyl-[1,1'-biphenyl]-4-amine) (Compound 3b): The synthetic route for **Compound 3b** followed the similar procedure for **Compound 3a** except changing the initial ratio of **Compound 1** to **Compound 2** from 1:2 to 1:1. A purple solid was gained at yield of 13.4%.

^{1}H NMR (400 MHz, Chloroform-*d*) δ 8.92 (ddd, *J* = 12.9, 8.1, 3.8 Hz, 8H), 8.25 (dd, *J* = 8.0, 2.3 Hz, 4H), 8.12 (d, *J* = 7.2 Hz, 4H), 7.93 (dd, *J* = 8.2, 2.1 Hz, 4H), 7.79 (d, *J* = 8.2 Hz, 4H), 7.56 (d, *J* =

7.6 Hz, 4H), 7.35 (d, J = 7.8 Hz, 4H), 7.32 (s, 4H), 7.30 (d, J = 8.3 Hz, 4H), 7.24 (d, J = 7.8 Hz, 8H), 7.10 (t, J = 7.3 Hz, 4H), 2.71 (s, 6H), -2.69 (s, 2H).

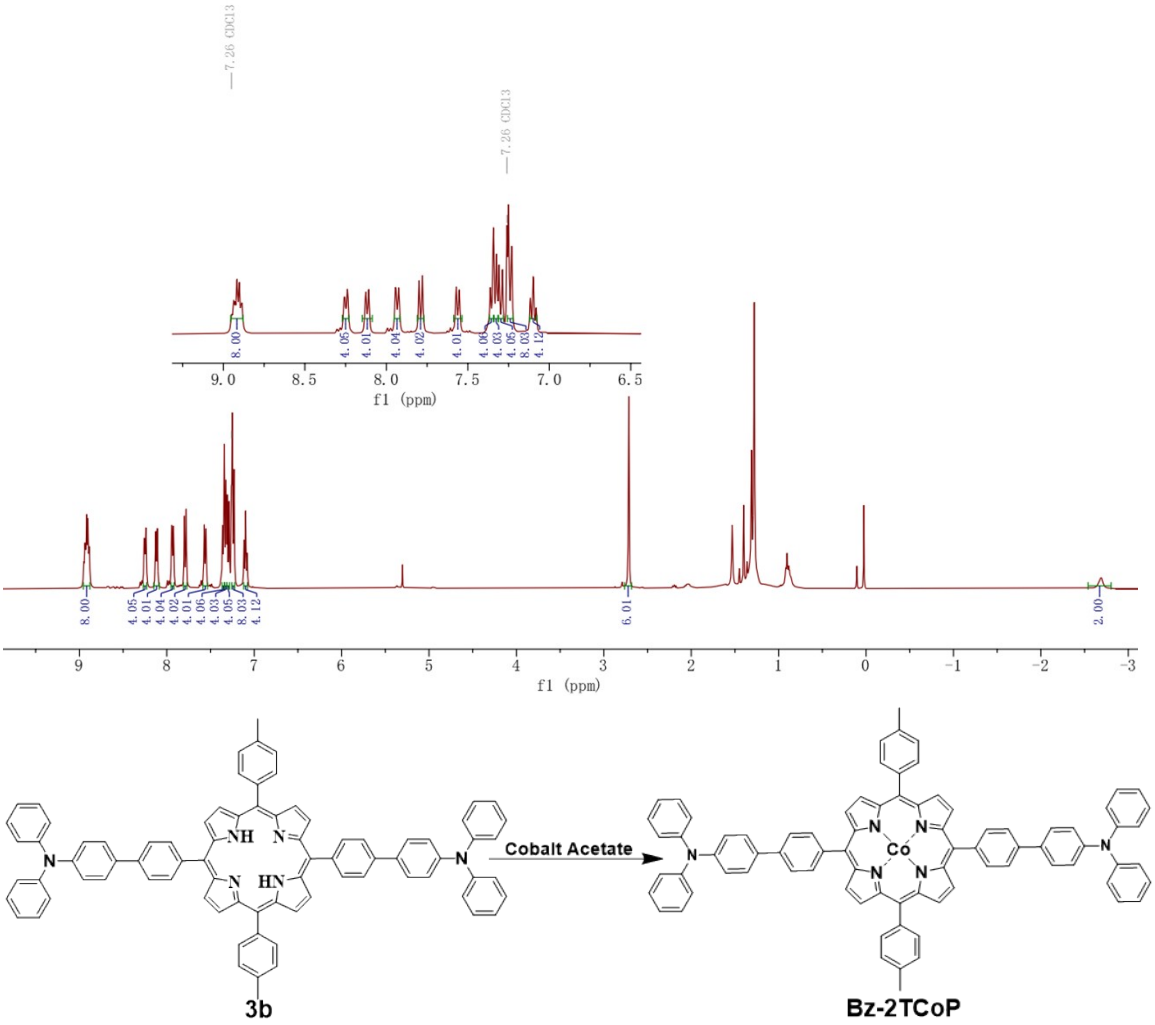

4',4'''-(5,15-di-p-tolylporphyrin-10,20-diyl) bis (N, N-diphenyl-[1,1'-biphenyl]-4-amine) cobalt (II) (Bz-2TCoP): The synthetic route for **Bz-2TCoP** followed the similar procedure for **aBz-TCoP** except changing the precursor **Compound 3a** to **Compound 3b**. A dark red solid was gained at yield of 89%.

HR-MS (m/z): requires for: $C_{80}H_{52}CoN_6$ 1085.4005, found $[M]^+$ = 1085.4080.

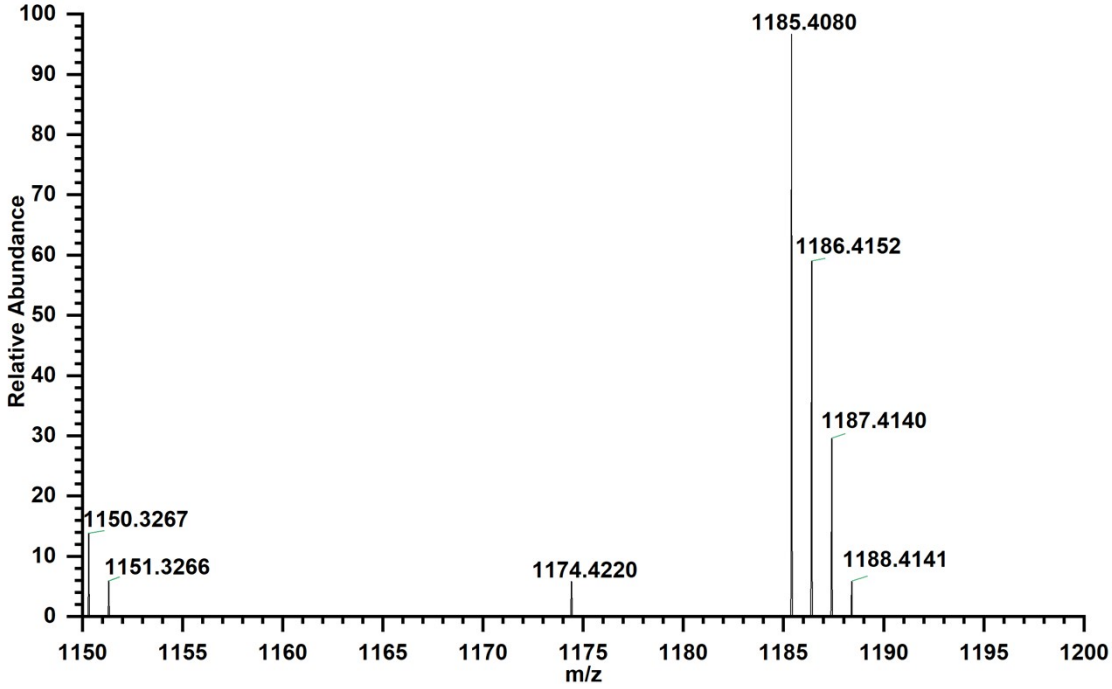
Relative Abundance
m/z
1185.4080
1186.4152
1187.4140
1188.4141
1150.3267
1151.3266
1174.4220
100
90
80
70
60
50
40
30
20
10
0
1150
1155
1160
1165
1170
1175
1180
1185
1190
1195
1200

SI 2. DFT results

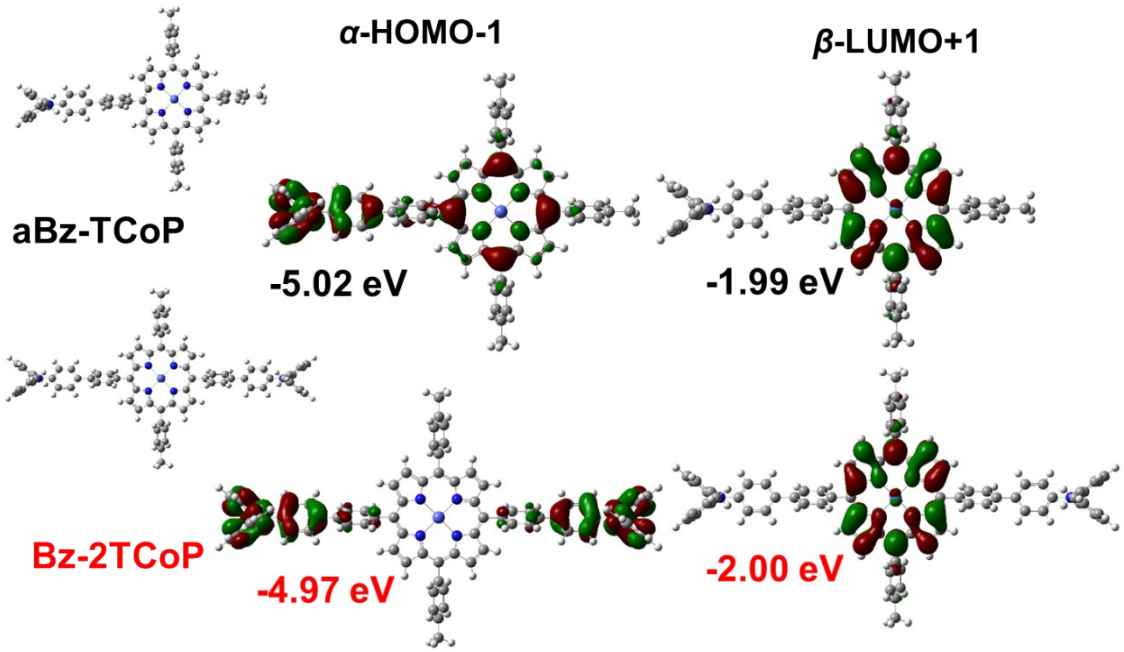

Figure S2. Optimized structures and DFT calculated higher energy molecular orbitals with energy levels of **aBz-TCoP** and **Bz-2TCoP**.

SI 3. UV-vis absorption spectra

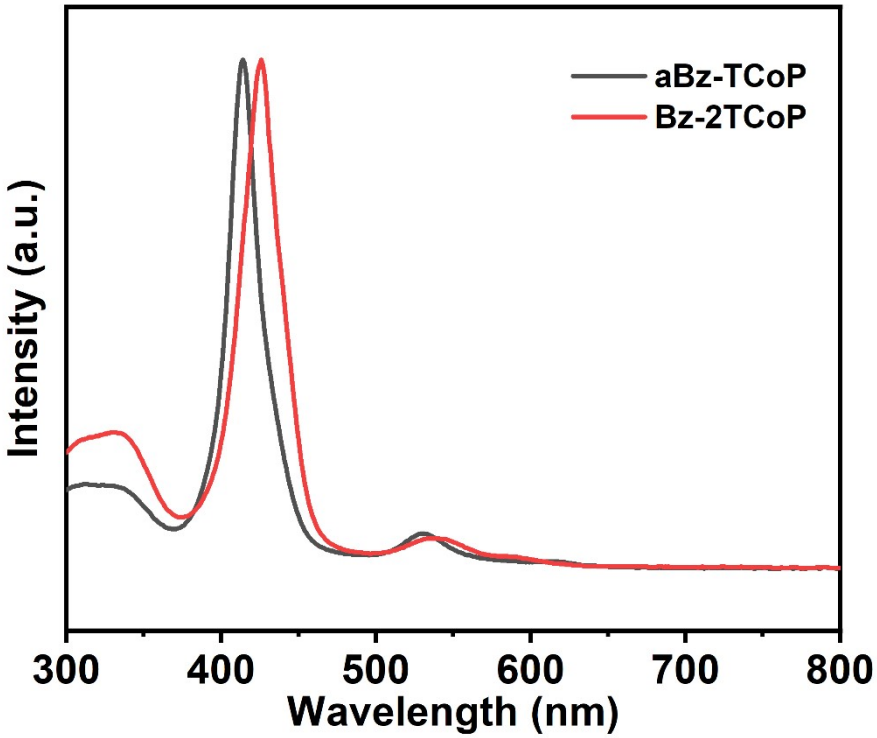

Figure S3. Normalized UV-vis absorption spectra of **aBz-TCoP** and **Bz-2TCoP** in DCM solution.

SI 4. IR spectra

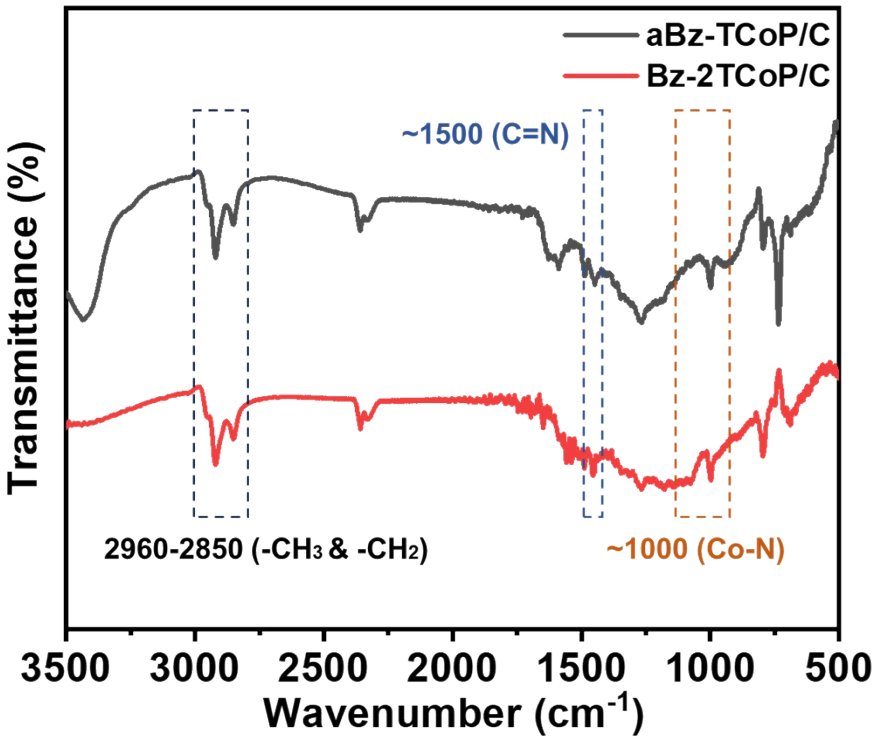

Figure S4. IR spectra of **aBz-TCoP/C** and **Bz-2TCoP/C**.

SI 5. Raman spectra

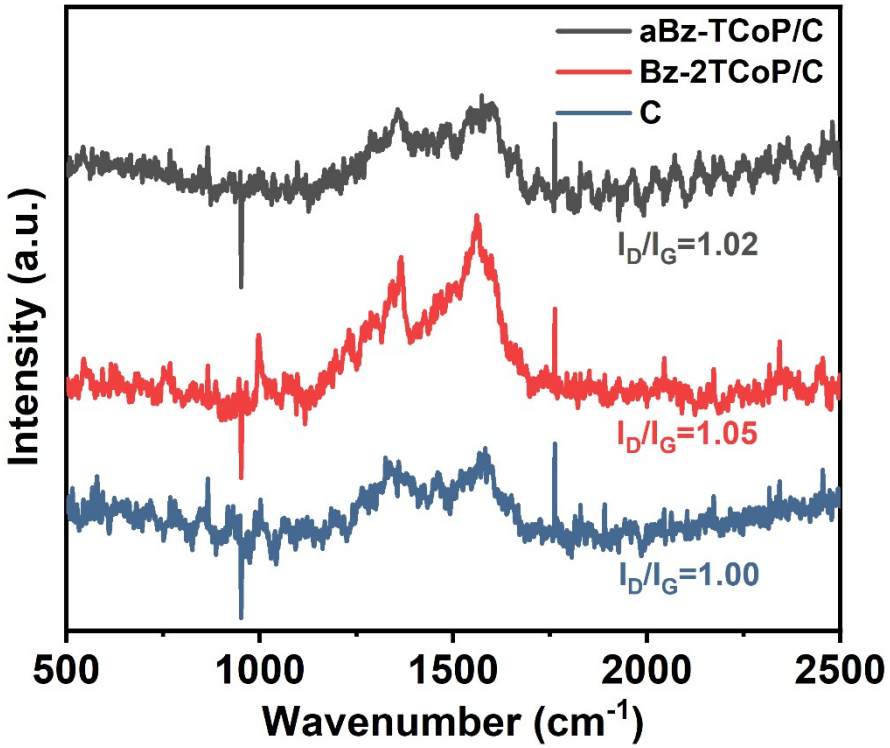

Figure S5. Raman spectra of **aBz-TCoP/C, Bz-2TCoP/C** and **Carbon black (C).**

SI 6. XPS

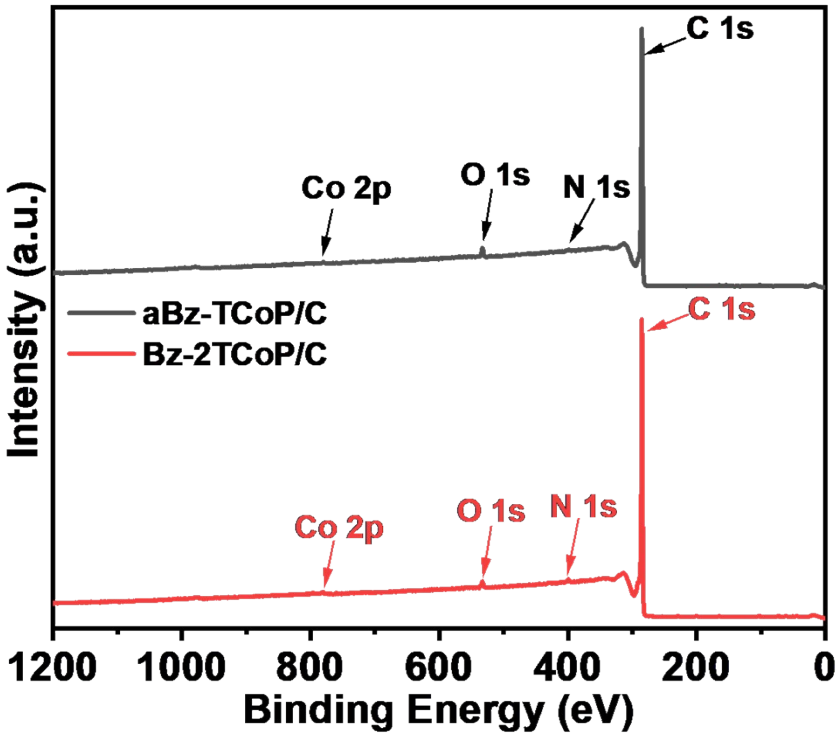

Figure S6. XPS survey spectra of **aBz-TCoP/C** and **Bz-2TCoP/C.**

SI 7. Electrochemical data of aBz-TCoP/C and Bz-2TCoP/C

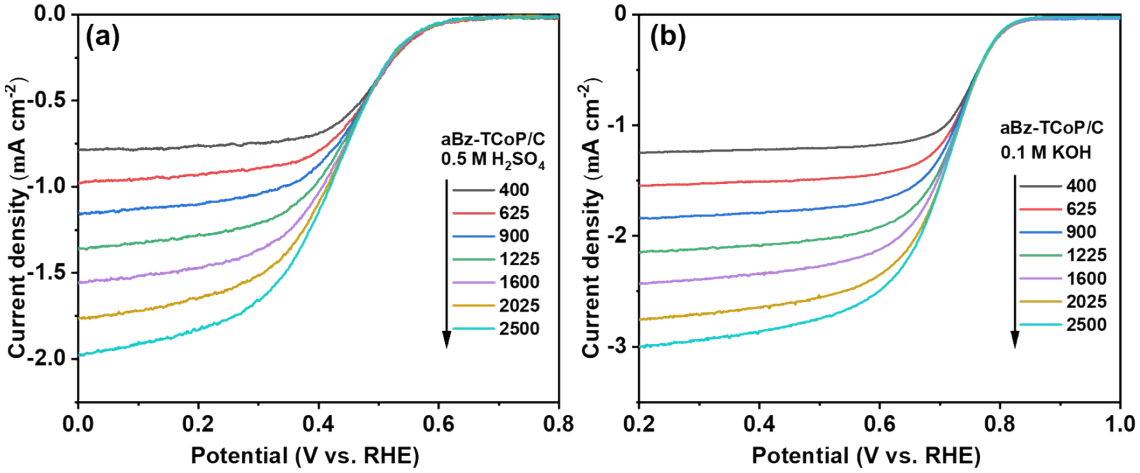

Figure S7. LSV plots of **aBz-TCoP/C** in O_2-saturated (a) 0.5 M H_2SO_4 and (b) 0.1 M KOH at various of rotation speeds. Scan rate: 10 mV s^{-1}.

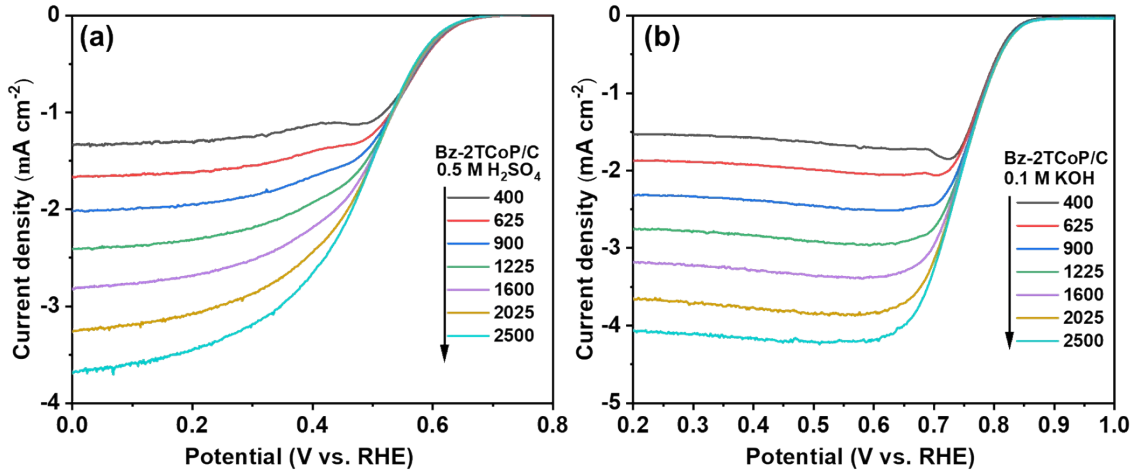

Figure S8. LSV plots of **Bz-2TCoP/C** in O_2-saturated (a) 0.5 M H_2SO_4 and (b) 0.1 M KOH at various of rotation speeds. Scan rate: 10 mV s^{-1}.

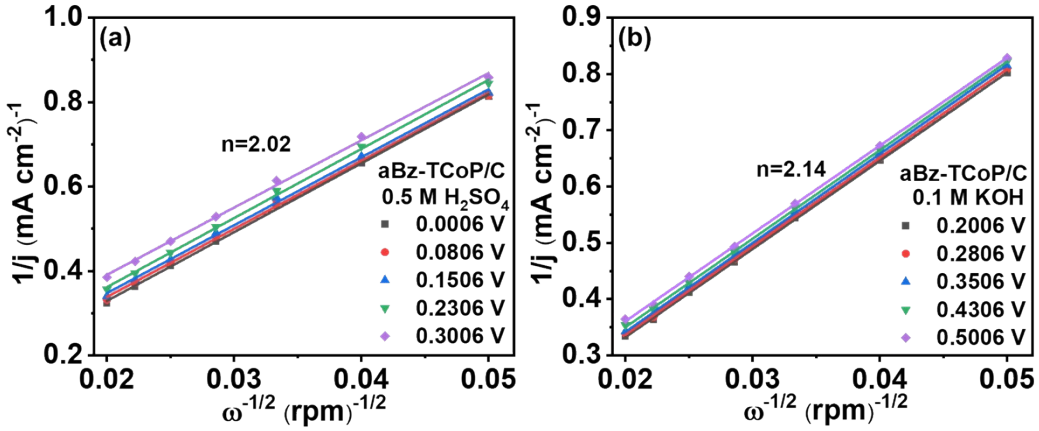

Figure S9. K-L plots of **aBz-TCoP/C** in O_2-saturated (a) 0.5 M H_2SO_4 and (b) 0.1 M KOH at various of rotation speeds.

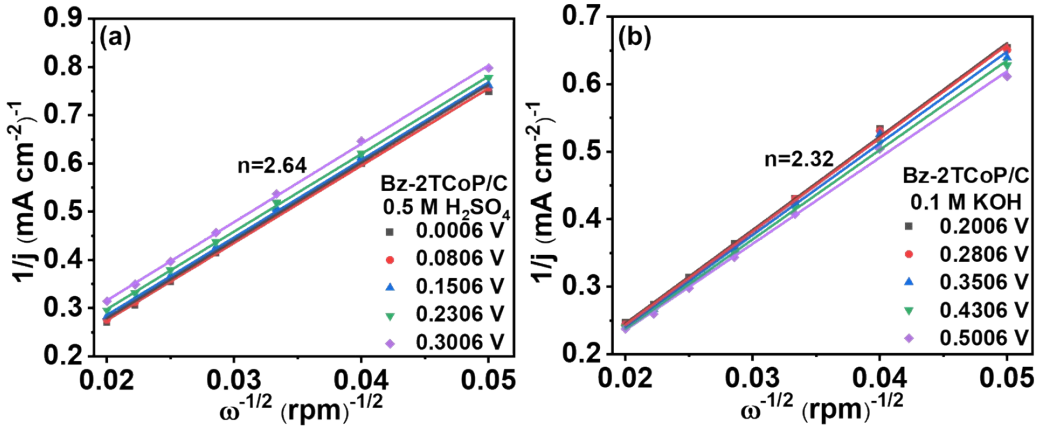

Figure S10. K-L plots of **Bz-2TCoP/C** in O_2-saturated (a) 0.5 M H_2SO_4 and (b) 0.1 M KOH at various of rotation speeds.

SI 8. Tafel diagrams of aBz-TCoP/C and Bz-2TCoP/C

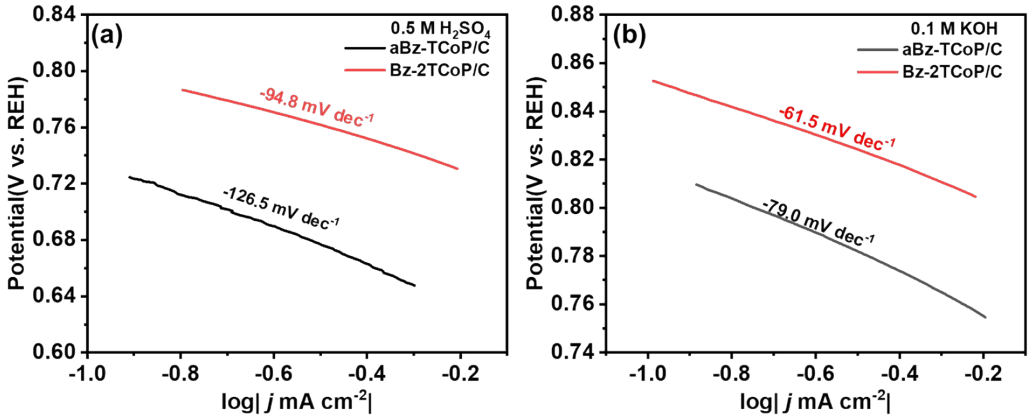

Figure S11. The corresponding Tafel diagrams of **aBz-TCoP/C** and **Bz-2TCoP/C** in O_2-saturated (a) 0.5 M H_2SO_4 and (b) 0.1 M KOH at 1600 rpm.

SI 9. Data of different metal loadings in aBz-TCoP/C

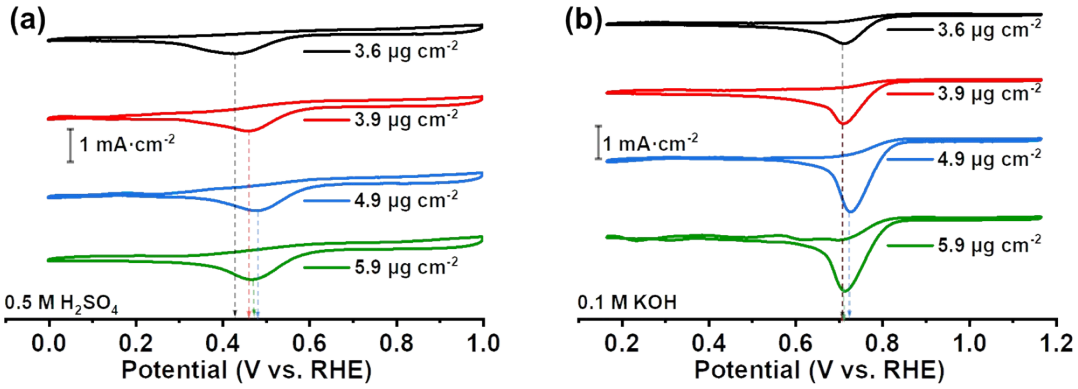

Figure S12. CV curves of **aBz-TCoP/C** with different cobalt loadings in O_2-saturated (a) 0.5 M H_2SO_4 and (b) 0.1 M KOH. Scan rate: 50 mV s^{-1}.

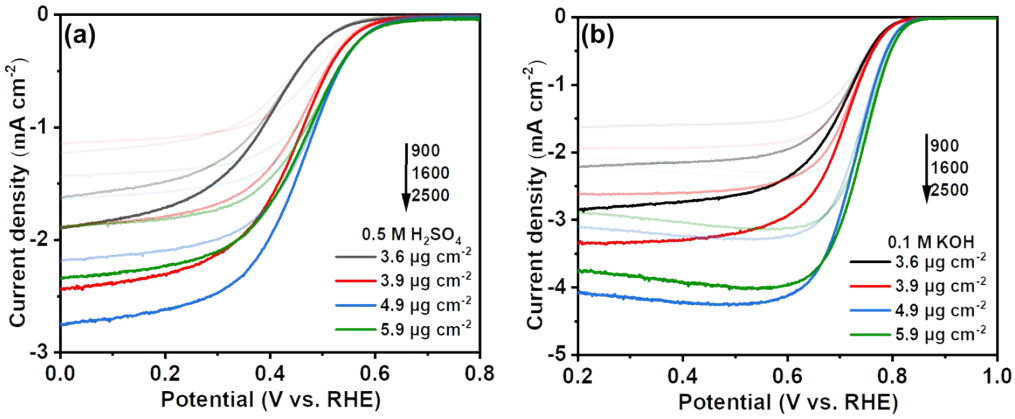

Figure S13. LSV plots of **aBz-TCoP/C** with different cobalt loadings in O_2-saturated (a) 0.5 M H_2SO_4 and (b) 0.1M KOH at different rotation speeds. Scan rate: 10 m V s^{-1}.

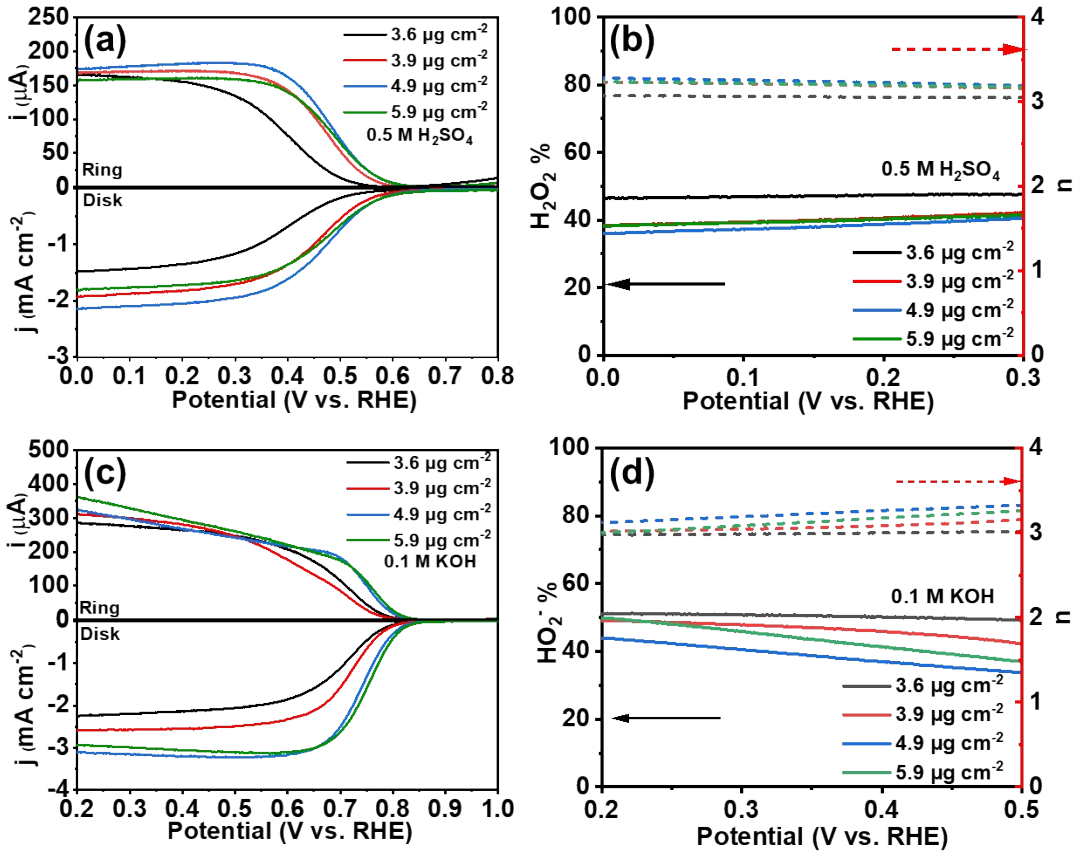

Figure S14. RRDE curves of **aBz-TCoP/C** with different cobalt loadings in O_2-saturated (a) 0.5 M H_2SO_4 and (c) 0.1 M KOH, and the corresponding H_2O_2% / HO_2^-% (solid lines) and *n* (dotted lines) values of **aBz-TCoP/C** at the recorded potential range in (b) 0.5 M H_2SO_4 and (d) 0.1 M KOH. Rotation speed: 1600 rpm. Scan rate: 10 m V s^{-1}.

SI 10. Comparison table of the cobalt porphyrin-catalytic ORR performance

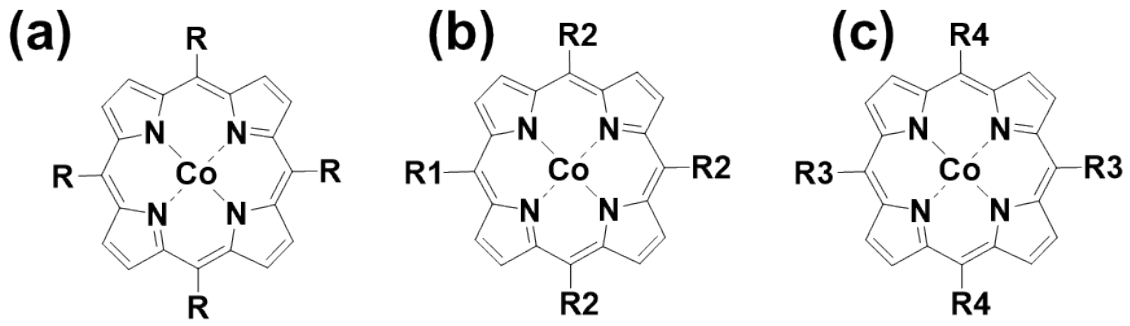

Figure S15. Template molecules for the comparison of ORR performance in Tables S1-3

Table S1. Summary of catalyst structure and ORR performance with Fig. S15a as the template molecules. All potentials are vs. RHE.

Catalysts	R structure	E_{ORR}[a] (V)	$E_{1/2}$[c] (V)	J_L[d] (mA cm^{-2})	n[e]	Solution	Reference
1@ZIF-67	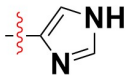	-	0.79	-	≈3.7	0.1 M KOH	[2]
(TPP)Co 1c	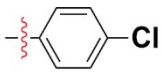	0.15	0.20	-	≈2.4	1.0M $HClO_4$	[3]
1/CNTs	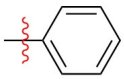	-	0.81	-5.46		0.1 M KOH	[4]

Table S2. Summary of catalyst structure and ORR performance with Fig. S15b as the template molecules. All potentials are vs. RHE.

Catalysts	R1 structure	R2 structure	E_{ORR}[a] (V)	n[e]	Solution	Reference
aBz-TCoP/C	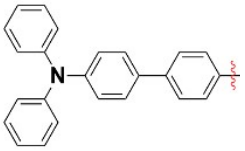		0.41	3.2	0.5 M H_2SO_4	**This work**
			0.70	3.0	0.1 M KOH	
CoHPX-1	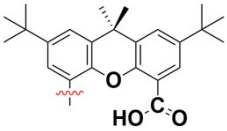	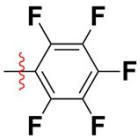	0.44	≈3.4	0.5 M H_2SO_4	[5]
A-TPA-CoPor	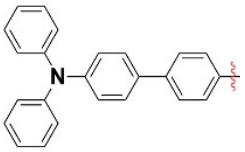	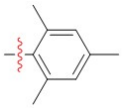	0.44	≈3.6	0.5 M H_2SO_4	[6]
			-	≈3.8	pH=0	
$CoTPPNMe_3^+$	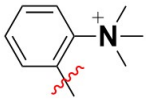		-	≈3.5	pH=4	[7]
			-	≈3.2	pH=7	

Table S3. Summary of catalyst structure and ORR performance with Fig. S15c as the template molecules. All potentials are vs. RHE.

Catalysts	R3 structure	R4 structure	$E_{1/2}$[c] (V)	J_L[d] (mA cm^{-2})	n[e]	Solution	Reference
Bz-2TCoP/C	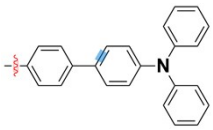		0.52	-2.82	3.6	0.5 M H_2SO_4	**This work**
			0.77	-3.18	3.5	0.1 M KOH	
XCP4@C	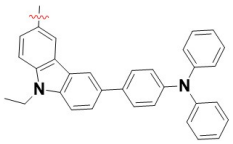		0.39	-1.64	≈2.5	0.5 M H_2SO_4	[8]
BCP1/C	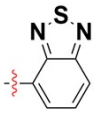		0.33	-1.75	≈3.0	0.5 M H_2SO_4	[9]
BCP2/C	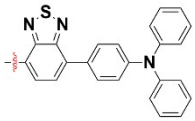		0.29	-1.96	≈2.3	0.5 M H_2SO_4	
s-TPA-CoP/XC	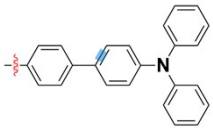		0.61	-4.19	≈3.1	0.1 M KOH	[10]
CN-CoPor/C	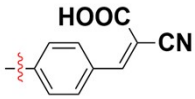		0.48	-2.52	≈3.2	0.5 M H_2SO_4	[11]
			0.71	-3.78	≈3.4	0.1 M KOH	
TPA-BTD-CoPor/C	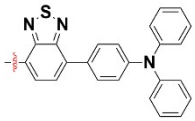		0.47	-3.78	≈3.0	0.1 M KOH	[12]

References

[1] T. Rohand, E. Dolusic, T.H. Ngo, W. Maes, W. Dehaen, Efficient synthesis of aryldipyrromethanes in water and their application in the synthesis of corroles and dipyrromethenes, ARKIVOC, 2007 (2007) 307-324.

[2] Z.Z. Liang, H.B. Guo, G.J. Zhou, K. Guo, B. Wang, H.T. Lei, W. Zhang, H.Q. Zheng, U.P. Apfel, R. Cao, Metal-Organic-Framework-Supported Molecular Electrocatalysis for the Oxygen Reduction Reaction, Angew Chem Int Edit, 60 (2021) 8472-8476.

[3] L.N. Ye, Y.Y. Fang, Z.P. Ou, S.L. Xue, K.M. Kadish, Cobalt Tetrabutano- and Tetrabenzotetraarylporphyrin Complexes: Effect of Substituents on the Electrochemical Properties and Catalytic Activity of Oxygen Reduction Reactions, Inorg Chem, 56 (2017) 13613-13626.

[4] S.L. Xue, W.R. Osterloh, X.J. Lv, N.C. Liu, Y.M. Gao, H.T. Lei, Y.Y. Fang, Z.T. Sun, P.F. Mei, D. Kuzuhara, N. Aratani, H. Yamada, R. Cao, K.M. Kadish, F.X. Qiu, Enhanced Four-Electron Oxygen Reduction Selectivity of Clamp-Shaped Cobalt(II) Porphyrin(2.1.2.1) Complexes, Angew Chem Int Edit, (2023).

[5] R. McGuire, D.K. Dogutan, T.S. Teets, J. Suntivich, Y. Shao-Horn, D.G. Nocera, Oxygen reduction reactivity of cobalt(II) hangman porphyrins, Chem Sci, 1 (2010) 411-414.

[6] R. Yuan, Y. Wei, B. Musikavanhu, M. Tang, Z. Xue, A. Wang, J. Zhang, X. Qiu, L. Zhao, Asymmetric cobalt porphyrins for oxygen reduction reactions: Boosted catalytic activity by the use of triphenylamine, Molecular Catalysis, 534 (2023).

[7] R. Zhang, J.J. Warren, Controlling the Oxygen Reduction Selectivity of Asymmetric Cobalt Porphyrins by Using Local Electrostatic Interactions, J Am Chem Soc, 142 (2020) 13426-13434.

[8] L. Zhao, Q.X. Xu, Z.W. Shao, Y. Chen, Z.L. Xue, H.N. Li, J.M. Zhang, Enhanced Oxygen Reduction Reaction Performance Using Intermolecular Forces Coupled with More Exposed Molecular Orbitals of Triphenylamine in Co-porphyrin Electrocatalysts, Acs Appl Mater Inter, 12 (2020) 45976-45986.

[9] Q.X. Xu, L. Zhao, Y.H. Ma, R. Yuan, M.S. Liu, Z.L. Xue, H.N. Li, J.M. Zhang, X.P. Qiu, Substituents and the induced partial charge effects on cobalt porphyrins catalytic oxygen reduction reactions in acidic medium, J Colloid Interf Sci, 597 (2021) 269-277.

[10] R. Yuan, Y.Q. Wei, Z.L. Xue, A.J. Wang, J.M. Zhang, H.J. Xu, L. Zhao, Effects of support material and electrolyte on a triphenylamine substituted cobalt porphyrin catalytic oxygen reduction reaction, Colloid Surface A, 665 (2023).

[11] Y.Q. Wei, L. Zhao, R. Yuan, Z.L. Xue, J. Mack, C. Chiyumba, T. Nyokong, J.M. Zhang, Promotion of Catalytic Oxygen Reduction Reactions: The Utility of Proton Management Substituents on Cobalt Porphyrins, Inorg Chem, 61 (2022).

[12] Q. Xu, L. Zhao, R. Yuan, Y. Chen, Z. Xue, J. Zhang, X. Qiu, J. Qu, Interfacial charge transfer mechanism of oxygen reduction reaction in alkali media: Effects of molecular charge states and triphenylamine substituent on cobalt porphyrin electrocatalysts, Colloid Surface A, 629 (2021).